EUROFUSION WPJET1-PR(16) 14757

G Sergienko et al.

Quartz micro-balance results of pulse-resolved erosion/deposition in the JET-ILW divertor

Preprint of Paper to be submitted for publication in
22nd International Conference on Plasma Surface Interactions
in Controlled Fusion Devices (22nd PSI)

This work has been carried out within the framework of the EUROfusion Consortium and has received funding from the Euratom research and training programme 2014-2018 under grant agreement No 633053. The views and opinions expressed herein do not necessarily reflect those of the European Commission.

Quartz micro-balance results of pulse-resolved erosion/deposition in the JET-ILW divertor

G. Sergienko[a], H.G. Esser[a], A. Kirschner[a], A. Huber[a], M. Freisinger[a], S. Brezinsek[a], A. Widdowson[b], Ch. Ayres[b], A. Weckmann[c], K. Heinola[d] and JET contributors*

EUROfusion Consortium, JET, Culham Science Centre, Abingdon, OX14 3DB, UK
[a]Forschungszentrum Jülich GmbH, Institut für Energie- und Klimaforschung – Plasmaphysik, Partner of the Trilateral Euregio Cluster (TEC), 52425 Jülich, Germany
[b]CCFE, Culham Science Centre, OX14 3DB, Abingdon UK
[c]Department of Fusion Plasma Physics, Royal institute of Technology (KTH),) 100 44 Stockholm, Sweden
[d]Department of Physics, University of Helsinki, P.O. Box 64, 00560 Helsinki, Finland
*See the Appendix of F Romanelli et al, Proceedings of the 25th IAEA Fusion Energy Conference 2014, Saint Petersburg, Russia

Abstract

A set of quartz crystal microbalances (QMB) was used at JET with full carbon wall to monitor mass erosion/deposition rates in the remote areas of the divertor. After introduction of the ITER- like wall (ILW) in JET with beryllium main wall and tungsten divertor, strong reduction of the material deposition and accompanied fuel retention was observed. Therefore the existing QMB electronics have been modified to improve the accuracy of frequency measurements by a factor of ten down to 0.1 Hz which corresponds to 1.4 ng/cm^2. In JET-ILW the averaged deposition rates of 1.2 - 3 ng/cm^2·s and erosion rates of 5.6 - 8.1 ng/cm^2·s were observed in the inner divertor with the inner strike point positions close to the bottom edge of vertical tile 3 and at the horizontal tile 4 respectively. The erosion with averaged rates of ≈2.1 ng/cm^2·s and ≈120 ng/cm^2·s were observed in the outer divertor for the outer strike point positions at tile 5 and tile 6 respectively.

1. Introduction

Plasma-wall interaction in fusion devices results in material erosion of the first wall, its migration and deposition. According to the present knowledge, tritium contained in the co-deposited layers, which are mainly formed in the remote areas, is responsible for the major part of the in-vessel tritium inventory. Control of the tritium inventory is one of most important issues for the development of fusion reactors with an acceptable level of environmental hazards. Material redistribution in tokamaks with carbon wall was investigated over decades and underlying physics has been well understood. Understanding of these processes in tokamaks with full metal first wall is important with respect to the ITER project. The quartz crystal microbalance (QMB) method is widely used in industrial and laboratory applications for the measurement of the deposition/erosion in real time. This method is based on the change of the resonance frequency of the quartz crystal oscillator due to the change of the areal mass density of the layer deposited on the quartz crystal surface. Unfortunately, the quartz crystal resonance frequency depends also on the crystal temperature and stress forces as well. To reduce the influence of the temperature changes on the deposition rate measurements, water cooled AT-cut quartz crystals are usually used. Alternatively, an additional quartz crystal resonator protected against deposition is used for the temperature compensation. Due to technical difficulties, water-cooled QMB systems are not possible to install in the divertor region of the JET tokamak. Therefore the second method with two identical quartz crystal resonators, for the sensing and for the temperature compensation, was applied [1].

2. Experimental set-up

A set of quartz crystal microbalances was used at JET with full carbon wall to monitor material erosion/deposition rates in the remote areas of the divertor [1-7]. After installation of the ILW in JET with beryllium main wall and tungsten divertor, a strong reduction (factor ~10) of the material deposition and accompanied fuel retention was observed [8-10]. Four QMB sensors with gold electrodes equipped with shutters and compensation quartz crystals (for reduction of temperature effects) were installed at the entrance to the louvers behind the lower vertical targets of the inner (QMB1, QMB2, QMB3 at same poloidal but different toroidal locations) and outer (QMB5) divertor as shown in figure 1. These remote areas are accessible by neutral particles only. The QMB1, QMB2, QMB3 and QMB5 have an identical construction. The QMB in-vacuo electronics is based on single BiCMOS ASIC chip from SINTEF which contains the quartz crystal sensor oscillator, the compensation quartz crystal oscillator, the reference quartz crystal oscillator and two double balanced mixers. The latter are used to generate the output signal of the difference between the frequencies of the reference and both the deposition and compensation sensing crystals [11]. All quartz crystals have a resonance frequency of about 6 MHz with the reference crystals having higher frequencies by about 10 kHz. This approach was used to reduce QMB system signal frequencies because the in-vacuo QMB electronic boards are connected to the ex-vessel QMB drive circuits by means of 6 m long thermocouple cables, which are able to transmit the signals only within 0 - 100 kHz frequency bandwidth. The frequency differences between sensor and compensation crystals were about 1000-1500 Hz before the measurements. The chip with the reference quartz crystal is mounted on a printed ceramic board and placed in a copper box with two ceramic D-sub plugs. The first plug is used to connect the power supply with the two signal lines. The common pin of the plug is connected to the copper box. The second plug is used to connect the sensor and compensation crystals. Both sensor and compensation crystals having diameters of 14 mm and thickness of 0.275 mm are mounted on another printed ceramic board attached to the lid of a separate copper box [4]. This copper box has an orifice in front of the sensor crystal. The QMB electronics box is plugged to the sensor box by means of special connector with reduced heat conductance. The box assembly is covered with two heat shields made of 1 mm thick stainless steel having the orifices in front of the sensor crystals. The copper box assemblies are electrically isolated from the heat shield but coupled to it by 100 kΩ resistor. Both shields are connected to the carrier rib having JET vessel ground. The 8 mm orifice in the inner heat shield is closed by metal mesh for electrical shielding which have the transmission of 88.5%. The outer heat shield orifice has a diameter of 11 mm. Taking into account that the quartz crystal sensor is recessed by 13.5 mm with respect to outer heat shield, the acceptance angle of the central part of the crystal can be found to be about 24° with respect to the normal of the crystal surface. The surfaces of the sensor crystal as well as the compensation crystal are oriented vertically and parallel to the toroidal magnetic field. The QMB drive circuits provide stable 5 V power supply and insulate the QMB signal lines from the JET vessel ground. The quartz crystals are not actively cooled and the temperature excursion of the quartz crystal sensor during the exposure time can easily reach the Curie temperature (573°C) after which permanent loss of their piezo-electric properties. Therefore,

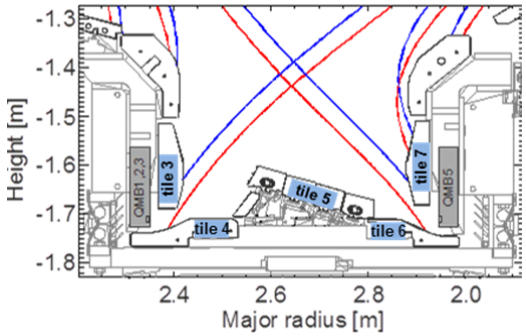

Fig.1. Positions of QMBs in divertor. Divertor magnetic field configurations: red line for strike points at the corners, blue line for strike points on the vertical targets.

the shutter opening time should be properly chosen taking into account the quartz sensor's distance to the strike point and additional heating power of the plasma.

The original JET QMB diagnostics [1] had frequency measurement accuracy of about 1-3 Hz, which was sufficient for carbon layers erosion/deposition measurement. To improve the accuracy of frequency measurements by a factor of ten down to 0.1 Hz (which corresponds to the areal density change about 1.4 ng/cm^2 or about 0.05 Be monolayer) the following modifications of the existing QMB electronics have been made: (i) all wired output of QMB in-vacuo electronic boards were connected to the QMB common input by 1 kΩ load resistors, to reduce electromagnetic noise pickup and protect the QMB circuit against electrostatic overvoltage, (ii) pulse width discriminators were installed in both measurement and reference QMB channels, which cut all noise pulses with duration below 0.005 ms , (iii) introduction of an electronical circuit for overheating protection of the measurement quartz crystal, which closes the electromagnetic shutter when the QMB sensor frequency drops below 4 kHz, which corresponds to the crystal temperature of about 220°C. The frequency measurements were performed with help of the pulse counting techniques. The time interval for the pulse counting was increased from 0.3-1 s to 10 s to provide 0.1 Hz accuracy. The QMBs frequencies as function of temperature were measured in laboratory by slow heating of the QMB assembly in vacuum oven. The results of these measurements were used to improve the compensation of the temperature effects. The quartz crystal mass sensitivity coefficient of 12.3 ng·cm^{-2}·Hz^{-1} was calculated using the Sauerbrey equation [12] and was confirmed by weight change measurements of the quartz sensors (the same type as used in JET QMB diagnostics) which were coated by different metal films (Cu, Cr and W) by means of magnetron sputtering. Taking into account the metal mesh transmittance, the mass sensitivity coefficient of 13.9 ng·cm^{-2}·Hz^{-1} was used for JET QMB data analysis.

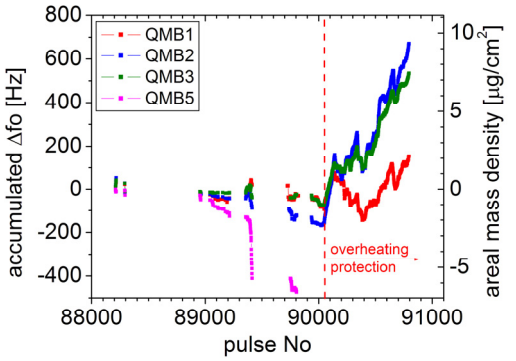

Fig.2. Accumulated frequency change versus plasma pulse

3. Experimental results and discussion

The quartz microbalance deposition monitors QMB1, QMB2, QMB3 and QMB5 were exposed to about 880, 836, 833 and 126 discharges respectively throughout the campaigns C36 in 2015-2016 during the divertor phase. These numbers of discharges correspond to 10230 s, 7172 s, 8646 s and 599 s respectively of total plasma exposure time. The pulse-resolved QMB measurements for all plasma pulses of the campaign are summarised in figure 2. The accumulated frequency change as a function of accumulated plasma exposure of the QMBs for these pulses is shown in figure 3. At the beginning of the campaign all QMBs were operated in manual mode (operator selects the shutters opening time). In most cases, the QMB shutters were opened for 1 - 2 s during divertor phase of the additional heated plasma.

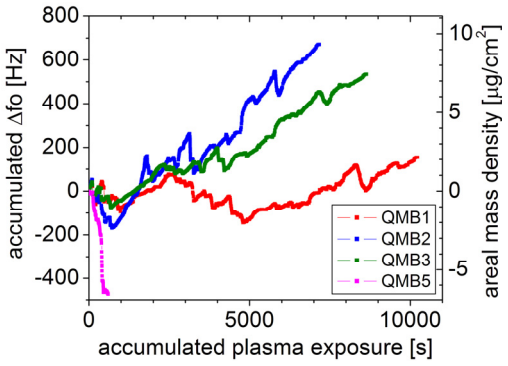

Fig.3. Accumulated frequency change versus accumulated plasma exposure of QMBs

The rather small opening interval has been chosen to avoid overheating of the sensing crystals. Starting from pulse #90051 the overheating protection circuits have been installed for the inner QMBs 1,2,3. The outer QMB5 was no longer operational at this time due to accidental overheating. After installation of the overheating protection circuits, the shutters were normally programmed to be opened 2 s before the start of the plasma discharge and the opening duration of 82 s, which is longer than the plasma discharge duration. The actual shutter closing times were defined by the quartz crystal sensor temperature. Due to this, the QMB exposures have been increased by a factor of 2.5 - 3.5. The different behavior of the QMB signals was observed for the initial phase of the campaign when the QMB exposure times were controlled manually and the final phase with longer exposure times of the QMBs and the automatic overheating protection in operation. Within the initial phase, in ohmic plasma discharges with the inner and outer strike points at the divertor corners or at the vertical targets, the QMBs installed in the inner divertor show deposition rates of up to 10 ng/cm^2·s. For the outer divertor under ohmic conditions, erosion rates of 2 - 6 ng·cm^{-2}·s^{-1} and deposition rates of 0.5 - 1.5 ng·cm^{-2}·s^{-1} were observed respectively for strike points at the divertor corners and at the vertical targets. All four QMBs detected erosion with rates of about 16 - 180 ng·cm^{-2}·s^{-1} during ion cyclotron resonance heating (ICRH) or NBI heated plasma discharges with the strike points at the divertor corners for both L-mode and H-mode plasmas.

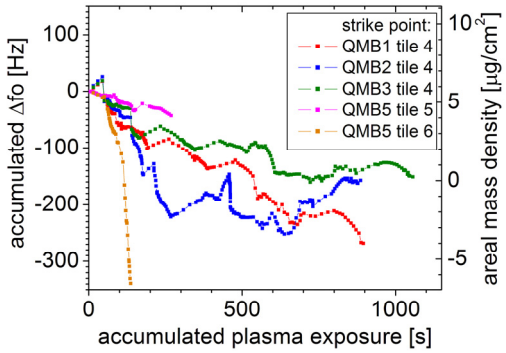

Fig.4. Accumulated frequency change versus accumulated plasma exposure of QMBs. The strike points on horizontal targets

The maximum erosion rates of about 150 ng·cm^{-2}·s^{-1} for the inner and of about 180 ng·cm^{-2}·s^{-1} for the outer divertor were observed in high power H-mode discharges with 17 MW NBI heating. With the strike points located at the vertical targets, deposition of about 0.75 - 4.5 ng·cm^{-2}·s^{-1} in the inner and erosion of about 1 - 10 ng·cm^{-2}·s^{-1} in the outer divertor were observed during both ICRH and NBI heating in L-mode plasmas. During the initial phase of the campaign with short QMB exposures net erosion for all inner divertor QMBs with mean rate of 1 - 4 ng·cm^{-2}·s^{-1} has been detected as seen in figure 3. The net erosion was observed by QMB5 with an average rate of about 18 ng·cm^{-2}·s^{-1}.

In the final phase, all inner divertor QMBs showed net deposition with averaged rates of 1.4 – 1.8 ng·cm^{-2}·s^{-1}. The QMB1 data sometime deviate from the QMB2 and QMB3 measurements probably due to increased dip activity (frequency jumps) of the compensation quartz crystal resonator. Remarkably, the deposition signals were frequently observed during NBI heated plasma with the strike points in the divertor corner - this was never seen in the initial phase of the campaign. This behavior is illustrated in figure 4 where the QMBs signals for the strike point positions at the horizontal targets (inner tile 4 or outer tile 6) are selected from the QMBs data shown on figure 3. During the first 200 s of plasma

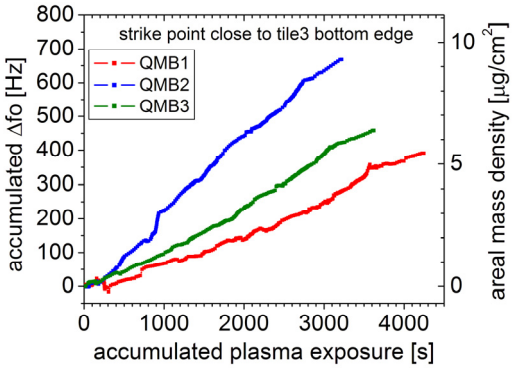

Fig.5. Accumulated frequency change versus accumulated plasma exposure of QMBs, strike point close to the bottom of vertical target (tile 3).

exposure all QMBs show stable erosion. The average erosion rate of 5.6 – 8.1 ng·cm^{-2}·s^{-1} was observed for the inner divertor QMBs. The average erosion rates of 24 – 120 ng·cm^{-2}·s^{-1} and 2.1 ng·cm^{-2}·s^{-1} respectively for the strike point at tile 6 and tile 5 were observed for the outer divertor QMB. The periods of the stable deposition appeared periodically for longer accumulated plasma exposures on the inner divertor QMBs with the rates of 4.7 – 19 ng·cm^{-2}·s^{-1}. Stable deposition with rates of 1.2, 3.0 and 1.7 ng·cm^{-2}·s^{-1} respectively for QMB1, QMB2 and QMB3 was observed on the inner divertor QMBs for the strike point positions at the bottom of the vertical target (tile 3) as seen on figure 5. The deposition rates for QMB2 were about a factor of 1.8 higher compared to QMB3 despite both were mounted at the divertor module 2 very close to each other. This can indicate that the particle flux to the QMB sensor has an essential toroidal component because QMB2 and QMB3 have only different shutter mountings with respect to the toroidal magnetic field, which can result in different shadowing.

The currently available data of JET-ILW show that under most conditions studied within the initial phase of the experimental campaign, the QMB signals indicate net erosion. This is in contradiction with post-mortem analysis of QMB crystals at the inner louvre from the first JET-ILW campaign [10] showing net layer deposition. In the first JET-ILW campaign the QMBs only delivered pulse-resolved measurements during the restart of the machine due to failure because technical issues. The shutters were afterwards opened to collect material until the end of the campaign for post-mortem analysis. In addition, previous QMB measurements in JET-C with full carbon wall [4] and ERO modelling for JET-C and also JET-ILW [13] show a clear dependence of QMB mass change regimes on the strike point position with largest deposition measured on the inner QMB when the inner strike point is located at the corner with direct line of sight to the QMB sensor. In contrast, the present measurements show largest erosion at the inner QMBs when the inner strike point is located at the corner. One possible explanation for the overall net erosion signals of the QMBs within the initial phase could be that the total mass balance is still dominated by the erosion of the initially clean gold electrodes due to fast neutrals. The possible simultaneous deposition flux of beryllium (and possibly also carbon, tungsten and oxygen) cannot be excluded but could be too small to be detectable against the much higher mass loss rate due to the gold erosion. This behavior had been changed within the final phase of the campaign because the gold electrode surface has been quickly covered by deposited light elements during prolonged QMB exposures. The fast neutrals responsible for the erosion likely originate from the reflection of high energetic D and/or Be ions from the target plates. An additional explanation for the erosion signals in the initial phase could be the change of the quartz resonance frequency due to stress caused by gold alloying with beryllium, which can change essentially tensile strength and ductility of the gold layer [14], and by the beryllium deposit itself. The latter would also explain the observed deviation of overnight QMBs frequency measurements from the sum of pulse based measurements shown on figure 6 for QMB3 which could be due to the stress relaxation. The slope of the pulse based QMB3 signal increases from negative value for plasma exposure below 700 s to values similar to the day based (measured

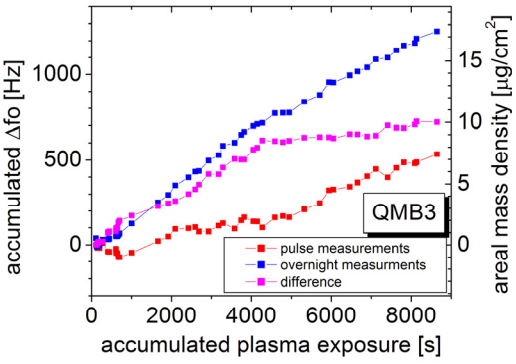

Fig.6. Accumulated frequency change versus accumulated plasma exposure of QMBs, strike point close to the bottom of vertical target (tile 3). Red curve for pulse based measurement, blue curve for overnight measurement in thermal equilibrium.

overnight) signal slope for exposures above 4300 s. The slope differences are nearly constant within the plasma exposure intervals of 0 - 700 s, 700 - 4300 s and 4300 - 8640 s and equal 0.21 Hz/s, 0.14 Hz/s and 0.031 Hz/s respectively. These slope differences can be also explained by the removal of the adsorbed gases from the deposit surface during plasma exposure which is followed by gas re-adsorption between the plasma pulses. Assuming the main desorbed gas is oxygen, the desorbed fluxes would be $7.8 \cdot 10^{12}$, $5.2 \cdot 10^{12}$ and $1.2 \cdot 10^{12}$ atom$\cdot$cm$^{-2}\cdot$s^{-1} which correspond to removal of less than 0.03 monolayer from the surface for 10 s plasma exposure. The later explanation is most probable because the reduction of the QMB exposure time from 2 s to 0.1 s did not essentially influence the large negative frequency change (about 2 Hz) during NBI heated plasma when the strike point was at the divertor corners such that the QMB was directly exposed to plasma VUV radiation and fast neutrals. The gas desorption can also explain the net erosion detected in final phase with strike point on the divertor corner shown in figure 4. Such behavior of the QMB signals was not observed in the full carbon divertor due to much higher deposition on QMBs in comparison with the adsorbed gas amount. The deposited layers in JET-ILW divertor are different in comparison with full carbon wall and consist on mainly beryllium with some amounts of oxygen, carbon and small traces of tungsten [4, 15]. This change of the deposited layer composition can also influence on the gas adsorption/desorption behavior. There is no direct view of the QMBs to the plasma when the strike point is on the vertical tile 3 therefore the day based deposition rate of about 2.2 ng$\cdot$cm$^{-2}\cdot$s^{-1} from the figure 6 is close to the pulse based deposition rate of 3.0 ng$\cdot$cm$^{-2}\cdot$s^{-1} because the pulse based measurement of the deposition rate should not be strongly affected by the gas desorption in this case.

4. Summary

The quartz microbalance deposition monitors QMB1, QMB2, QMB3 and QMB5 were exposed to about respectively 880, 836, 833 and 126 discharges throughout the campaigns C36 during the divertor phase. These correspond to respectively 10230 s, 7172 s, 8646 s and 599 s of total plasma exposure time.

The inner divertor QMBs measured net erosion during the first 200-250 plasma pulses with short opening times (1 - 2 s) exposed to additionally heated diverted plasmas. After extending of the shutter opening time by a factor of 2.5 - 3.5 (with including both ohmic and additionally heated phase of the plasma discharge), all inner divertor QMBs start to show net deposition with averaged rates between 1.2 and 3 ng$\cdot$cm$^{-2}\cdot$s^{-1} when the strike point position is close to the bottom edge of the vertical target (tile 3).

Net erosion was found on both the inner and outer divertor QMBs for strike points on the horizontal targets with rates of 5.6 – 8.1 ng$\cdot$cm$^{-2}\cdot$s^{-1} and 24 – 120 ng$\cdot$cm$^{-2}\cdot$s^{-1} respectively. The averaged erosion rate of 2.1 ng$\cdot$cm$^{-2}\cdot$s^{-1} was observed in the outer divertor for the strike point at tile 5.

The observation of net erosion during divertor corners configuration can be explained by: (i) erosion of the gold electrode on quartz crystal sensor; (ii) stress in the beryllium deposit, (iii) desorption-adsorption of the vacuum background gases on the deposited layer.

Acknowledgments

This work has been carried out within the framework of the EUROfusion Consortium and has received funding from the Euratom research and training programme 2014-2018 under grant agreement No 633053. The views and opinions expressed herein do not necessarily reflect those of the European Commission.

References

[1] H.G. Esser, G. Neill, P. Coad et al., Fus. Eng. Design 66–68 (2003)855

[2] H.G. Esser, V.Philipps, M. Freisinger et al., J. Nucl. Mater. 337–339 (2005) 84
[3] J.P.Coad, H.G. Esser, J. Likonen et.al., Fus. Eng. Design 74 (2005)745
[4] H.G. Esser, V. Philipps, P. Wienhold et al., J. Nucl. Mater. 363–365 (2007) 146
[5] H.G. Esser, A. Kreter, V. Philipps et al., J. Nucl. Mater. 390–391 (2009) 148
[6] A. Kreter, S. Brezinsek, J.P.Coad et al., J. Nucl. Mater. 390–391 (2009) 38
[7] A. Kreter, H.G. Esser, S. Brezinsek et al., Phys. Rev. Lett. 102(4) (2009) 045007
[8] S. Brezinsek et al., J. Nucl. Mat. 463 (2015) 11
[9] S. Brezinsek, A. Widdowson, M. Mayer et al., Nucl. Fusion 55 (2015) 063021
[10] H.G. Esser, V. Philipps, M. Freisinger et al., J. Nucl. Mat. 463 (2015) 796
[11] O. Vermesan, T. Rispal and L. Soulier, Low power ASIC for high temperature applications, High-Temperature Electronic Materials, Devices and Sensors Conference, 1998, San Diego, CA, 1998, pp. 81- 85
[12] G. Sauerbrey, Zeitschrift fiir Physik 155 (1959) 206
[13] A. Kirschner, D. Matveev, D. Borodin et al., J. Nucl. Mat. 463 (2015) 116
[14] B. Brenner, N.J. Tenafly, P. White et al., Beryllium-Gold Alloy and Article Made Therefrom, United States Patent, US 3272625 (1966)
[15] P. Petersson, M. Rubel H.G. Esser et al., J. Nucl. Mat. 463 (2015) 814